THE JOURNAL OF PHYSICAL CHEMISTRY B

pubs.acs.org/JPCB Article

Controlling the Rotational Barrier of Single Porphyrin Rotors on Surfaces

Qiushi Zhang,* Rui Pang, Tengfei Luo, and Michel A. Van Hove*

Cite This: J. Phys. Chem. B 2020, 124, 953–960 Read Online

ACCESS | Metrics & More | Article Recommendations | Supporting Information

ABSTRACT: Artificial molecular machines have played an indispensable role in many chemical and biological processes in recent decades. Among all kinds of molecular machines, molecular rotor systems have attracted increasing attention. In this work, we used density functional theory (DFT) calculations to investigate the rotational behaviors of on-surface molecular rotors based on porphyrin, which is a species of molecule with wide biological and chemical compatibilities. Moreover, our comparative studies demonstrate that macrocycle metalation, supporting substrate replacement, and functional group substitutions can effectively modify the rotational barrier of porphyrin rotors. We believe that these modification methods can further guide the path to achieve highly controllable on-surface molecular rotor systems in future applications.

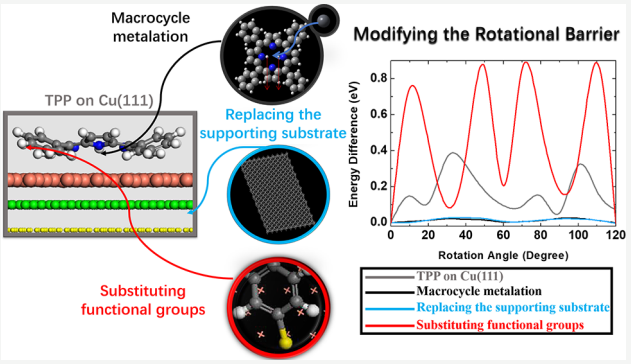

INTRODUCTION

In nature, molecular machines play a unique role in a wide range of chemical and biological processes.[1−5] Molecular rotors[6−9] are a class of nanoscale machines that can convert external energy, i.e., light,[10,11] chemical energy,[12−14] electricity,[6,15,16] etc., into controllable rotational motion. Molecular rotors have attracted special attention in recent decades because they are the fundamental components of larger integrated molecular machines.[17−19] Cyclic tetrapyrrole porphyrins are an important kind of chemical compounds in many biochemistry reactions.[20−23] The flexibility in the molecular geometry of porphyrins opens many opportunities for engineering their functional properties.[24−28] In recent years, many researchers have focused on porphyrins, including their molecular luminescence,[29−31] molecular spintronics,[32−35] and on-surface chemical reactions.[36] Porphyrins are known as a building block in common biological processes such as oxygen transport in mammalian heme and oxidation reactions in photosynthetic chlorophyll.[20,22] Therefore, the nontoxicity and adaptability of porphyrins are great advantages in future biochemistry applications.

Porphyrins adsorbed on solid supporting substrates are reported as an ideal system to investigate the behaviors of on-surface molecular rotors.[37−42] Their strong rotor−substrate coupling and their propeller shape make this adsorption system quite robust during rotational motion. The main advantage of porphyrin adsorption systems is that their rotational motion is highly controllable and easy to characterize experimentally.[37−42] In addition, porphyrins are chemically active with a variety of geometric distortions,[25,28,43] which allows for modifying rotational barriers feasibly. This provides opportunities to engineer the properties of porphyrin-based rotational systems according to real application needs. Furthermore, on-surface self-assembled two-dimensional molecular structures of porphyrins[44,45] can also be used to study the transfer of rotation between molecular gears.[46,47] In most cases, the strong porphyrin−substrate coupling induces relatively large rotational barriers,[28,37] which implies that the rotational motion cannot occur spontaneously at room temperature. To excite and control the rotation of porphyrin molecules adsorbed on substrates, many experimental methods have been utilized. For instance, electrical pulses in scanning tunneling microscopy (STM) were applied to excite the rotation of porphyrin molecules on metallic substrates in the investigations of Y. Zhang et al.[42] and H. Tanaka et al.[41] In addition, the adsorption site and orientation of porphyrins or other similar molecules with ring structures can be easily manipulated by STM tip.[32,48] As a result, STM-tip manipulation is considered to be another approach to manage the rotation of adsorbed porphyrin rotors. Other methods like inserting chemical ligands[40] and shining light[10,11] were also employed to excite the rotation. The rotational motion of porphyrins adsorbed on substrates can be easily characterized by surface-probing methodologies, such as STM.[40−42]

Received: October 23, 2019
Revised: January 3, 2020
Published: January 20, 2020

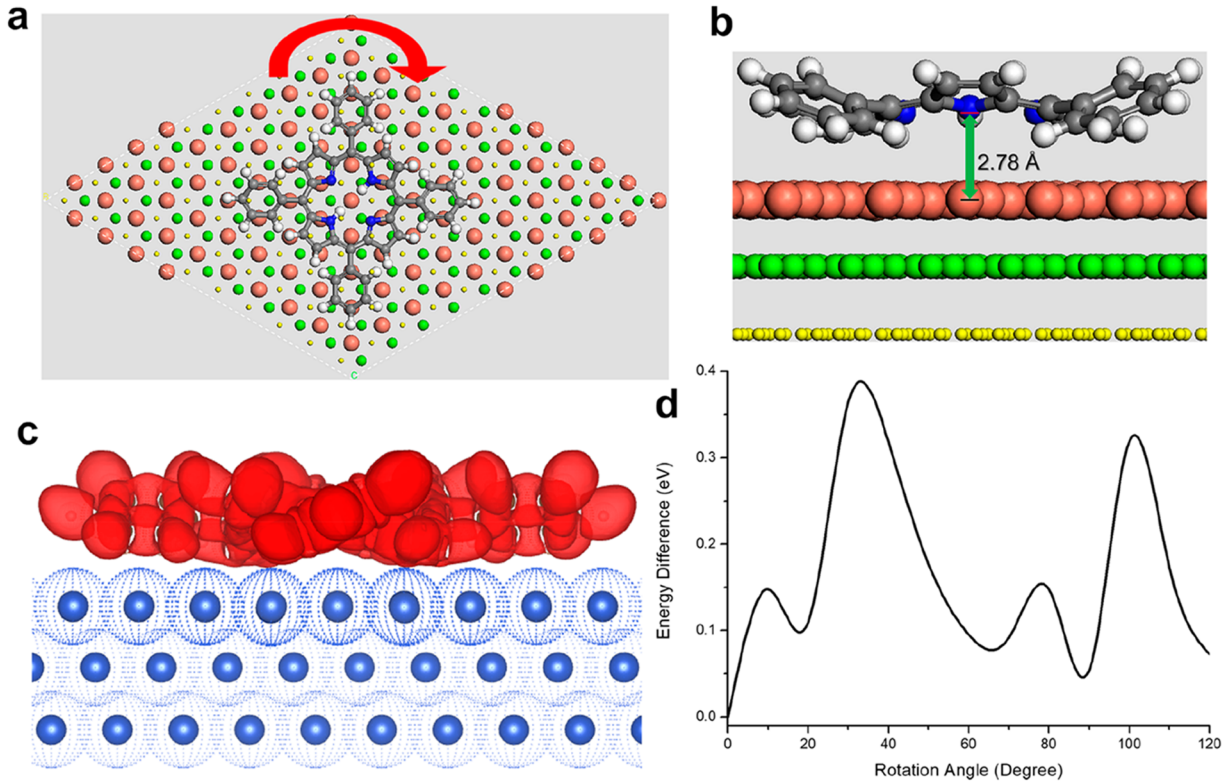

Figure 1. (a) Top view and (b) side view of the DFT-optimized geometry of a single TPP molecule adsorbed on a Cu(111) substrate. Hydrogen, carbon, and nitrogen atoms are identified in white, gray, and blue, respectively. The top (large, red), middle (medium, green), and bottom (small, yellow) layers of the copper atoms in the Cu(111) substrate are shown in different sizes and colors. The direction of rotation (clockwise) is identified by a curved red arrow. The adsorption height (defined in the text) is 2.78 Å and marked by a green arrow. (c) Electron localization function (ELF) of the TPP/Cu(111) system (Isosurface level: 0.65; red for TPP, blue for Cu(111)). (d) Rotational energy barrier (REB) of the TPP/Cu(111) system, for rotation from 0 to 120°. The energy difference is set to 0 at the 0° point.

Herein, we report our density functional theory (DFT) calculation investigations on some potential approaches to modify the rotational barrier of single porphyrins adsorbed on surfaces. The rotational barrier is a key property for molecular rotor systems. For our porphyrin rotors, the rotational barrier mainly originates from the adsorption coupling, primarily the van der Waals force, between porphyrins and substrates.[28,49−51] Most studies on porphyrin rotors are mainly focused on probing or exciting the rotational motion, while exploration of ways to control or even modify the properties of porphyrin rotors is still insufficient. In order to fulfill future application needs, the capability to increase or decrease the rotational barrier is indispensable. In our work, we have investigated the value of several approaches, specifically center-core metalation as well as supporting substrates and functional groups replacement. It turns out that all of these approaches are efficient for tuning the rotational barrier of single porphyrin rotors. These provide feasible choices to engineer the rotational barrier and speed of molecular rotors in future applications.

COMPUTATIONAL DETAILS

Our density functional theory (DFT) calculations were performed using the Vienna ad initio Simulation Package (VASP)[52,53] with the ion−electron interaction described by the projector-augmented wave potential (PAW). We employed an optimized version of the van der Waals (vdW) density functional (optB88-vdW) to describe the interaction between porphyrin molecules and substrates.[28,32,45,54,55] For the substrates Cu(111) and graphite(0001), a 10 × 10 unit-cell system (see Supporting Information, SI3) with three atomic layers was employed. During geometry optimization, only the outermost substrate layer was relaxed, while the deeper two layers were kept fixed (see Supporting Information, SI2). A vacuum layer of 20 Å was used to minimize the impact of the periodic slab structure. All the structural optimizations employed γ-point-only K-point sampling. While for the rotational barrier, electron localization function, and adsorption energy calculations, 4 × 4 × 1 K-point sampling and a Gaussian broadening of 0.02 eV were used. The plane-wave cutoff energy was 500 eV in all the calculations. The structures were found to be stable with all the atomic forces down to 10^{-2} eV/Å.

RESULTS AND DISCUSSION

First, we introduce the system of a single 5,10,15,20-tetraphenylporphyrin (TPP) molecule adsorbed on a Cu(111) substrate. On one hand, this basic model can give us a comprehensive understanding of the behaviors of porphyrin-based single molecular rotors on metallic substrates. On the other hand, it can also serve as the reference for a later comparison of the modified systems. Figure 1a displays the optimized geometry of the TPP/Cu(111) system. Such TPP/Cu(111) models are quite common and robust, and their fundamental properties have been well studied in many works.[56,57] Figure 1b shows a side view of our optimized

https://dx.doi.org/10.1021/acs.jpcb.9b09986
J. Phys. Chem. B 2020, 124, 953−960

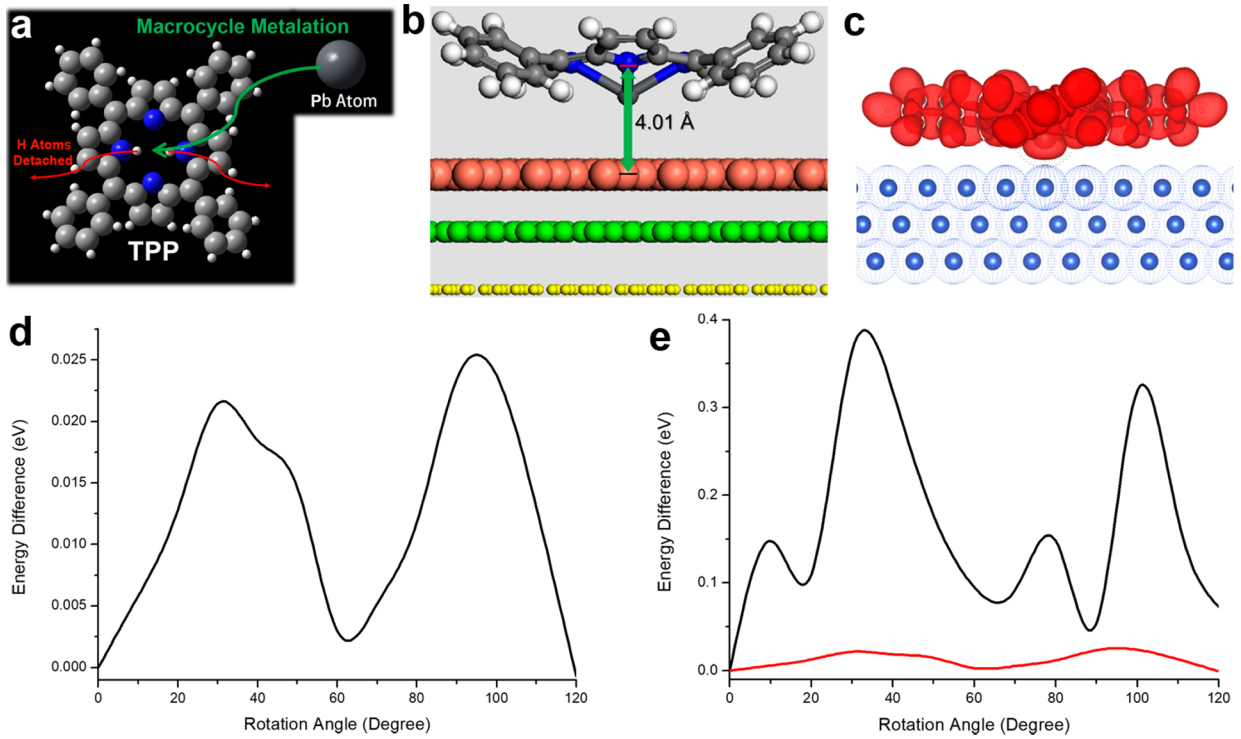

Figure 2. (a) Schematic diagram of the macrocycle metalation process with a Pb atom, colored dark gray. (b) Side view of the DFT-optimized geometry of a single Pb-TPP molecule adsorbed on a Cu(111) substrate. The adsorption height is 4.01 Å and marked by a green arrow. (c) ELF of the Pb-TPP/Cu(111) system (isosurface level: 0.65). (d) REB of the Pb-TPP/Cu(111) system, from 0 to 120°. The energy difference is set to 0 at the 0° point. (e) Comparison of the REB plots of TPP (black) and Pb-TPP (red) on Cu(111) with the same energy scale.

geometry. The TPP molecule adopts a saddle distortion with its four phenyl rings rotated into propeller-like orientations. This saddle distortion is totally different from the gas-phase geometry of TPP, which is planar: the saddle distortion originates from the strong rotor−substrate coupling, while the saddle feature can increase the stability of the system.[28,56,57] The adsorption height is 2.78 Å, as measured from the center of the nitrogen ring to the nuclear plane of the nearby top-layer copper atoms (see Figure 1b). This adsorption height is consistent with previous experimental results and indicates the existence of strong coupling between TPP and Cu(111).[28,57,58] To further interpret the strength of rotor−substrate coupling, the adsorption energy (E_{ads}) was calculated by the following formula:

$$E_{ads} = E_{sub+mol} - E_{mol} - E_{sub} \quad (1)$$

where $E_{sub+mol}$ is the total energy of the fully optimized and complete adsorption system, E_{mol} is the energy of the gas-phase relaxed molecular rotor, and E_{sub} is the energy of the relaxed substrate after removal of molecular rotor. The adsorption energy for the TPP/Cu(111) system is calculated as −4.06 eV. The electron localization function (ELF) of this adsorption system is depicted in Figure 1c, with an isosurface level of 0.65. Both the adsorption energy and the ELF plot evidence the strong electronic interaction between the TPP molecule and the Cu(111) substrate.[59]

To simulate the rotation process, we started with the stable orientation of TPP on Cu(111), which has the lowest total energy. Then, we "manually" rotated the TPP molecule clockwise by 10° about the center perpendicular axis (as shown in the Supporting Information, SI1) while keeping the molecular geometry unchanged. Next, we reoptimized the entire system while freezing the four center nitrogen atoms to maintain the imposed rotation. By repeating this rotation-reoptimization process, we produce the rotational energy barrier (REB) of the TPP/Cu(111) system. The REB plot of TPP/Cu(111) is shown in Figure 1d. The averaged magnitude of the two main rotational barriers is around 0.36 eV; the barriers differ due to the symmetry breaking induced by the three-fold rotational symmetry of Cu(111) (see Supporting Information, SI4). Since the rotational barrier is quite large, the rotational motion of TPP on Cu(111) cannot be spontaneous near or below room temperature, and this rotational motion is normally excited by STM-tip manipulation or an external electrical field in experiments. The low symmetry in the REB curve is mainly due to the fact that it is hard to perfectly match the center of mass of the saddle-distorted porphyrin rotors with the symmetry axes of the substrates in the computational models. Thus, porphyrin rotors may be slightly off-center during the entire rotation process. In addition, the strong rotor−substrate coupling can also cause slight deformation and off-centering of porphyrin rotors and atom displacements in substrates during rotation.

We next explored modifications of our single porphyrin rotor. The first modification, macrocycle metalation or tetrapyrrole metalation,[60−62] originally appeared in nature: it allows metalloporphyrins to be synthesized. Macrocycle metalation is very important, since a large variety of properties, including chemical, electronic, and magnetic, can be introduced by metalloporphyrins, which in turn enhances their functionality in metabolic catalysis, molecular electronics, and photovoltaics.[63] As illustrated in Figure 2a, free-base porphyrins and metal atoms are initially mixed on substrates or in solutions. With proper annealing conditions, the tetrapyrrole

https://dx.doi.org/10.1021/acs.jpcb.9b09986
J. Phys. Chem. B 2020, 124, 953−960

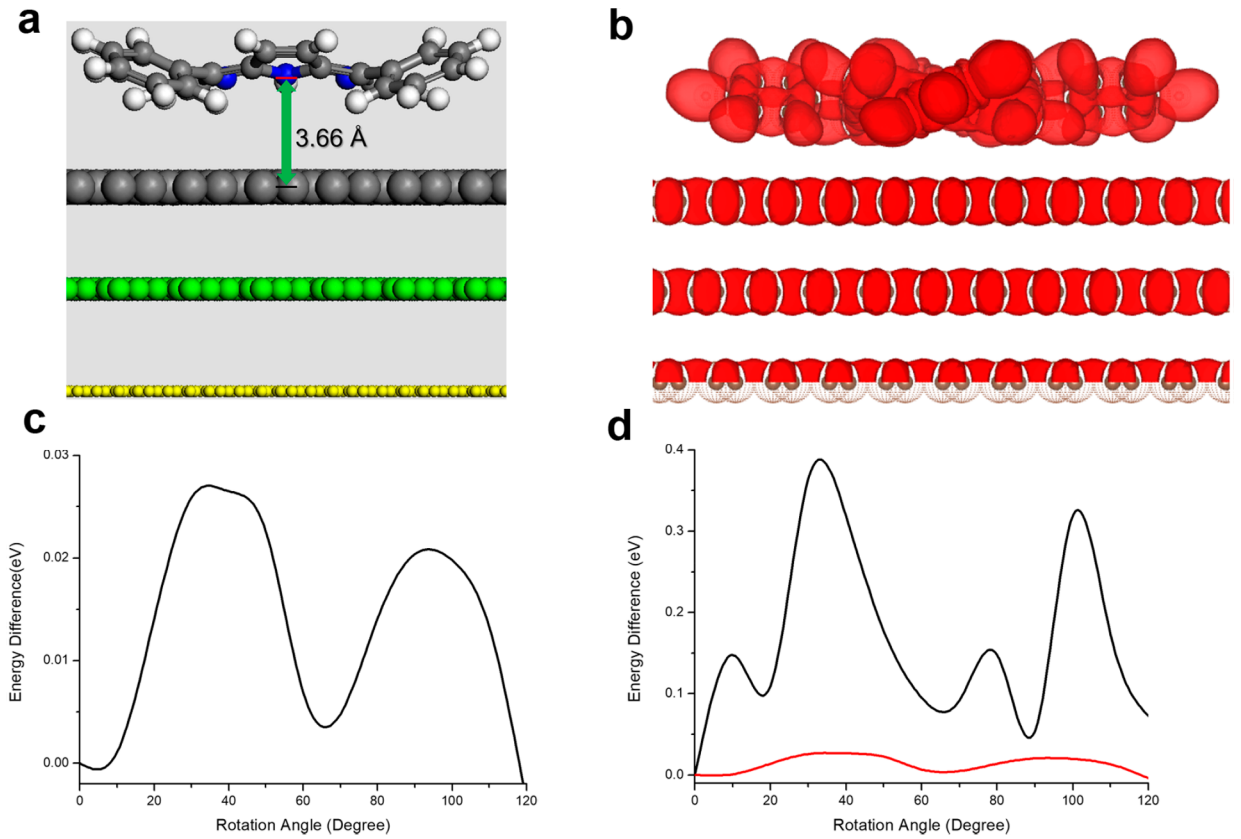

Figure 3. (a) Side view of the DFT-optimized geometry of a single TPP molecule adsorbed on a graphite(0001) substrate. The adsorption height is 3.66 Å and marked by a green arrow. (b) ELF of the TPP/graphite(0001) system (isosurface level: 0.65). (c) REB plot of the TPP/graphite(0001) system, from 0 to 120°. The energy difference is set to 0 at the 0° point. (d) Comparison of the REB plots of TPP on Cu(111) (black) and on graphite(0001) (red) with the same energy scale.

core can be self-metalated by the predeposited metal atoms while the central two hydrogen atoms detach from the nitrogen atoms. Experimental methods, like surface-enhanced resonant Raman spectroscopy[64,65] and STM,[69] have been used to probe the occurrence of macrocycle metalation. In vacuo surface-supported metalation is one of the effective ways to synthesize metalloporphyrins on substrates, and thus, it is considered to be a good way to synthesize on-surface metalloporphyrin rotors.[63]

Many species of metal atoms can be used in macrocycle metalation.[63] In addition to commonly used Fe, Co, Ni, Mn, and Zn atoms, porphyrin- or phthalocyanine-based molecules can also be effectively metalated by atoms with a larger atomic size, like Pb or Bi atoms.[66−69] We used lead (Pb) atoms and TPP in the metalation on Cu(111), resulting in the Pb-TPP/Cu(111) molecular rotor system. Due to the large atomic size of the Pb atom, two configurations of Pb-TPP can be found on the substrate after macrocycle metalation, with the Pb atom sitting above or below the molecular plane.[68,69] We select the configuration of the Pb atom below the molecular plane as our single molecular rotor. This is because this configuration preferentially adsorbs as isolated molecules on most metallic substrates, and the Pb atom below can bond to the Cu atom in the supporting substrate as a joint. As shown in Figure 2b, Pb-TPP, like normal TPP, also prefers a saddle conformation on Cu(111) after full optimization. This means that the existence of rotor−substrate coupling can still stabilize the molecular rotor system and provide a rotational barrier. Because of the large Pb atom inserted between TPP and the Cu(111) substrate, the adsorption height of Pb-TPP is increased to ∼4 Å, around 1.2 Å higher than in the TPP/Cu(111) system. In addition, the decoupling effect of the Pb atom can also be visualized from the weakened electronic interaction between molecular rotor (Pb-TPP) and the Cu(111) substrate, as shown in the ELF graph in panel c (Figure 2). As a result, the adsorption energy of Pb-TPP on Cu (111) is decreased to −3.35 eV, which is 0.7 eV lower than for TPP on Cu(111).

Even though the inserted Pb atom decouples the molecular rotor from the substrate, it still can work as a connection and a rotational axle for our rotor system (see Figure 2c). Figure 2d presents the REB plot of Pb-TPP on Cu(111), which is calculated by using the same method as described in the last section. As displayed in the plot, the averaged rotational barrier of Pb-TPP is about 0.023 eV. To directly compare the rotational barriers of Pb-TPP/Cu(111) and TPP/Cu(111) systems, we present the REB plots of these two systems on the same scale in Figure 2e. It is obvious that the rotational barrier decreased by more than 10-fold after the metalation of the Pb atom. Therefore, we find that macrocycle metalation can be a very effective method to modify the rotational barrier of single porphyrin rotors on surfaces. This modification strategy can inspire future research on studying the relation between the rotational behaviors of porphyrin rotors and macrocycle metalation by many different kinds of metallic atoms.

As we discussed above, the rotational barrier of an on-surface molecular rotor system originates from the coupling between the molecular rotor and substrate. In the last section, we introduced an effective modification, Pb-atom macrocycle

https://dx.doi.org/10.1021/acs.jpcb.9b09986
J. Phys. Chem. B 2020, 124, 953−960

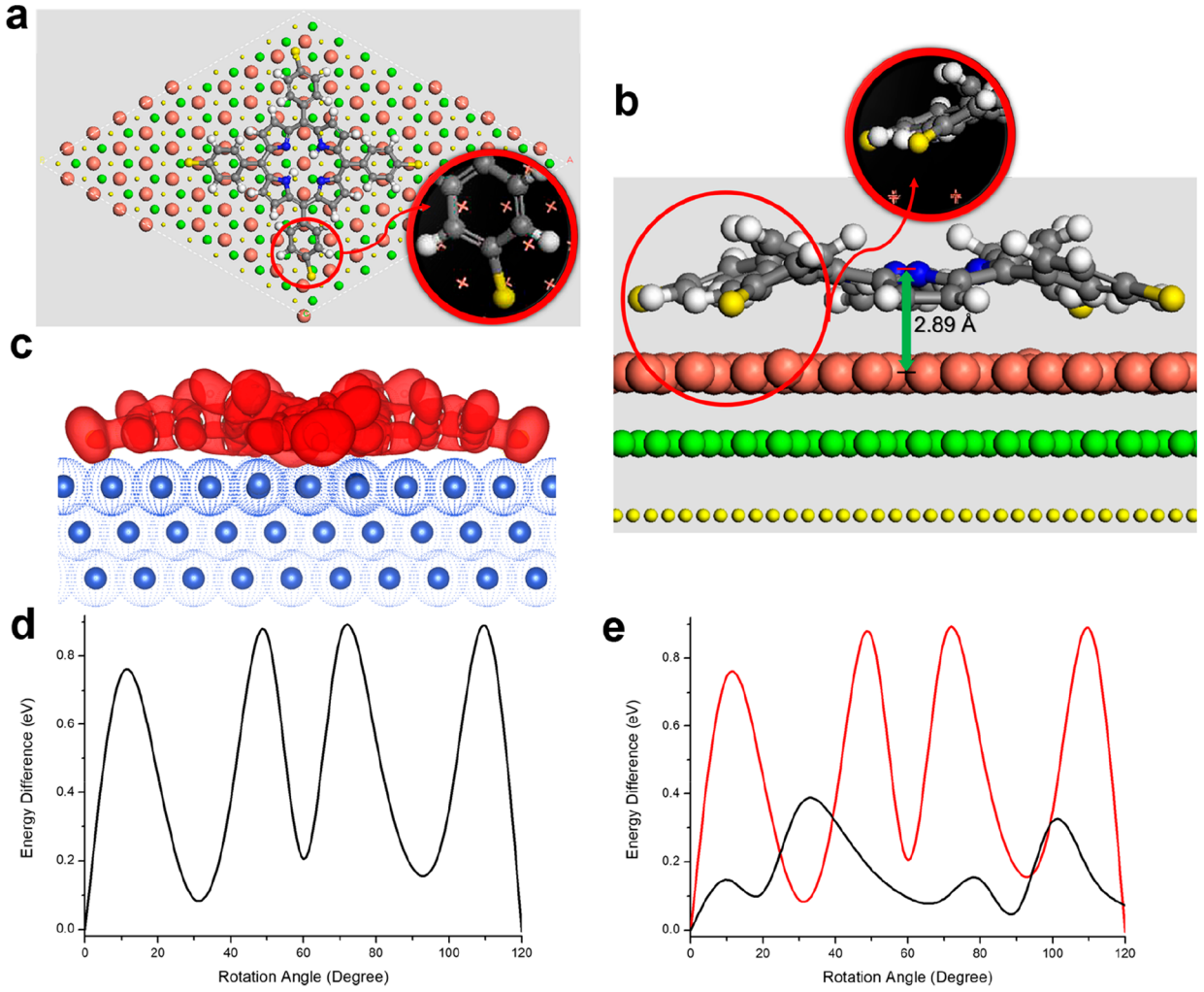

Figure 4. (a) Top view and (b) side view of the DFT-optimized geometry of a single S_4TPP molecule adsorbed on a Cu(111) substrate. Sulfur atoms are identified in yellow. The adsorption height of S_4TPP is 2.89 Å, which is marked by a green arrow. The insets zoom in on the tilting and downward bending of the sulfur atoms. (c) ELF of the S_4TPP/Cu(111) system (isosurface level: 0.65). (d) REB of the S_4TPP/Cu(111) system, from 0 to 120°. The energy difference is set to 0 at the 0° point. (e) Comparison of the REB plots of TPP (black) and S_4TPP (red) on Cu(111) with the same energy scale.

metalation, of the molecular rotor. Next, we instead modify the substrate. Porphyrin molecules can adsorb strongly on many metallic substrates, like Cu(111) and Au(111).[28,34,50,56−58] Here, we replace the Cu(111) substrate with graphite(0001) to weaken the rotor−substrate coupling. For a direct comparison, we still choose a single TPP molecule as our rotor. On the basis of previous works, porphyrins adsorbed on graphite or graphene substrates can still form stable adsorption systems[70−73] with a relatively lower molecule−substrate coupling strength compared with many metallic substrates.[73,74]

Similar to the TPP/Cu(111) system, we used three layers of a carbon honeycomb lattice as our graphite(0001) substrate, relaxing the top layer and freezing the two deeper layers during geometry optimization (see Figure 3a). The optimized conformation of a single TPP on graphite(0001) is presented in Figure 3a. The single TPP molecule again prefers a saddle distortion due to the rotor−substrate coupling, which is very similar in magnitude to the adsorption on Cu(111) before and after metalation; however, the adsorption height is now 3.66 Å, which is ∼0.9 Å higher than in the TPP/Cu(111) system. The adsorption energy of TPP/graphite(0001) is also much lower than that of the TPP/Cu(111) system, which is around −2.92 eV, and even lower than that of the Pb-TPP/Cu(111) system. Figure 3b displays the ELF of the TPP/graphite(0001) system. Compared with the ELF of the TPP/Cu(111) system (Figure 1c), the electronic interaction between the rotor and substrate is much weaker (less electronic overlap) in the TPP/graphite(0001) system. This is mainly due to the increased rotor−substrate distance and the different shell structure of graphite substrate. On the basis of the increased adsorption height, lower adsorption energy, and weaker electronic interaction in the TPP/graphite(0001) system, we can deduce that the rotational barrier of TPP/graphite(0001) will be lower than for the TPP/Cu(111) system. This is confirmed by the REB plot of the TPP/graphite(0001) system shown in Figure 3c. The averaged magnitude of the rotational barrier is calculated as 0.025 eV. Again, the rotational barrier of TPP/graphite(0001) is more than 10-fold smaller than in the TPP/Cu(111) system. Figure 3d compares the rotational barriers of the TPP/graphite(0001) and TPP/Cu(111) systems. It is obvious that the rotational barrier of TPP/graphite(0001) is much lower than that of the TPP/Cu(111) system. On the basis of the results for the TPP/graphite(0001) system, we find that replacing the substrate can be another very effective

https://dx.doi.org/10.1021/acs.jpcb.9b09986
J. Phys. Chem. B 2020, 124, 953−960

method for modifying the rotational barrier of the on-surface porphyrin rotor system.

In the previous two sections, we have introduced two potential modification methods, macrocycle metalation and substrate replacement, which can effectively reduce the rotational barrier of single porphyrin rotors on surfaces. However, in order to fulfill practical application needs, increasing the rotational barrier may also be desirable. In this section, we will discuss one way to achieve this. The hydrogen atoms on the side phenyl rings or the side phenyl rings themselves on the porphyrin macrocycle can be replaced by many other kinds of atoms or functional groups. The resulting systems not only can be very robust but also can have greatly enhanced rotor−substrate interactions.[28,43,75,76] Utilizing this property, we choose sulfur atoms to replace the four hydrogen atoms on the four side phenyl rings of TPP and obtain a S_4TPP molecular rotor. Because the four sulfur atoms in S_4TPP are not saturated by hydrogen atoms, each has one unpaired electron. These unpaired electrons can strongly enhance the rotor−substrate interaction and increase the rotational barrier.

The optimized molecular geometry (top view) of S_4TPP on Cu(111) is shown in Figure 4a. The whole adsorption system is quite stable after geometry optimization, and S_4TPP has a saddle distortion, which is similar to the previous cases. When we zoom into the optimized geometry of S_4TPP, we find two special features: the sulfur atoms are tilted and bent down toward the substrate (see the insets in Figure 4a and b). Due to this displacement of the sulfur atoms, the average adsorption height of the four sulfur atoms (2.08 Å) is ∼0.8 Å less than the adsorption height of the porphyrin macrocycle (2.89 Å), as shown in Figure 4b. Since the interaction between the four sulfur atoms and the substrate is very strong (also see the ELF graph in Figure 4c), they have greatly enhanced the overall rotor−substrate interaction. As a result, the adsorption energy of S_4TPP/Cu(111) is much higher than in the previous cases, namely about −12.54 eV. Figure 4d shows the REB plot of the S_4TPP/Cu(111) system. The average rotational barrier of S_4TPP/Cu(111) is about 0.75 eV, which is more than double that of the TPP/Cu(111) system. This significant increase of rotational barrier can be clearly visualized in the comparison of the REB plots in Figure 4e. Therefore, we can find that replacing the atoms or functional groups on porphyrin rotors can significantly modify the rotational barrier with high freedom as well.

CONCLUSIONS

To summarize, using DFT calculations, we first investigated the rotational motion of a porphyrin molecular rotor, TPP, on a metallic substrate, Cu(111). Moreover, our comparative studies show that macrocycle metalation and substrate replacement are both very effective modification methods that can greatly reduce the rotational barrier of porphyrin rotors, namely by an order of magnitude. On the other hand, we also demonstrate that substituting the functional groups attached on the porphyrin enables the rotational barrier to be more than doubled. Therefore, our studies provide several effective modification methods to achieve highly controllable on-surface molecular rotor systems in future applications. These modification strategies can also inspire further research in this field.

ASSOCIATED CONTENT

Supporting Information

The Supporting Information is available free of charge at https://pubs.acs.org/doi/10.1021/acs.jpcb.9b09986.

Schematics of the rotational methodology, demonstration of the second substrate layer relaxation in geometry optimization, coverage effect information, and information on the rotational symmetry of Cu(111) substrate (PDF)

AUTHOR INFORMATION

Corresponding Authors

Qiushi Zhang − *Institute of Computational and Theoretical Studies & Department of Physics, Hong Kong Baptist University, Hong Kong SAR, China; Department of Aerospace and Mechanical Engineering, University of Notre Dame, Notre Dame 46556, Indiana, United States;* orcid.org/0000-0003-1313-7965; Email: qzhang12@nd.edu

Michel A. Van Hove − *Institute of Computational and Theoretical Studies & Department of Physics, Hong Kong Baptist University, Hong Kong SAR, China;* orcid.org/0000-0002-8898-6921; Email: vanhove@hkbu.edu.hk

Authors

Rui Pang − *International Laboratory for Quantum Functional Materials of Henan, Zhengzhou University, Zhengzhou 450001, China*

Tengfei Luo − *Department of Aerospace and Mechanical Engineering, University of Notre Dame, Notre Dame 46556, Indiana, United States;* orcid.org/0000-0003-3940-8786

Complete contact information is available at: https://pubs.acs.org/10.1021/acs.jpcb.9b09986

Notes

The authors declare no competing financial interest.

ACKNOWLEDGMENTS

We acknowledge financial support from the Collaborative Research Fund of the Research Grants Council of Hong Kong (Grant No. C2014-15G). We acknowledge the High Performance Cluster Computing Centre (HPCCC) in Hong Kong Baptist University and the Tianhe-2 cluster at the National Supercomputer Center in Guangzhou, China for providing the computational resources. ICTS and HPCCC are supported by the HKBU Institute of Creativity, which is sponsored by the Hung Hin Shiu Charitable Foundation. We also acknowledge financial support from the National Science Foundation (1706039), Post-Doctor Foundation (2019M652559), and the National Natural Science Foundation Youth Project (11704342).

REFERENCES

(1) Browne, W. R.; Feringa, B. L. Making molecular machines work. *Nat. Nanotechnol.* **2006**, *1*, 25−35.

(2) Bath, J.; Turberfield, A. J. DNA nanomachines. *Nat. Nanotechnol.* **2007**, *2*, 275−284.

(3) Carter, N. J.; Cross, R. A. Mechanics of the kinesin step. *Nature* **2005**, *435*, 308−312.

(4) Goel, A.; Vogel, V. Harnessing biological motors to engineer systems for nanoscale transport and assembly. *Nat. Nanotechnol.* **2008**, *3*, 465−475.

(5) Uchihashi, T.; Iino, R.; Ando, T.; Noji, H. High-speed atomic force microscopy reveals rotary catalysis of rotorless F_1-ATPase. *Science* **2011**, *333*, 755−758.
(6) Tierney, H. L.; Murphy, C. J.; Jewell, A. D.; Baber, A. E.; Iski, E. V.; Khodaverdian, H. Y.; McGuire, A. F.; Klebanov, N.; Sykes, E. C. H. Experimental demonstration of a single-molecule electric motor. *Nat. Nanotechnol.* **2011**, *6*, 625−629.
(7) Perera, U. G. E.; Ample, F.; Kersell, H.; Zhang, Y.; Vives, G.; Echeverria, J.; Grisolia, M.; Rapenne, G.; Joachim, C.; Hla, S.-W. Controlled clockwise and anticlockwise rotational switching of a molecular motor. *Nat. Nanotechnol.* **2013**, *8*, 46−51.
(8) van Delden, R. A.; ter Wiel, M. K. J.; Pollard, M. M.; Vicario, J.; Koumura, N.; Feringa, B. L. Unidirectional molecular motor on a gold surface. *Nature* **2005**, *437*, 1337−1340.
(9) Peplow, M. The tiniest lego: a tale of nanoscale motors, switches and pumps. *Nature* **2015**, *525*, 18−21.
(10) Koumura, N.; Zijlstra, R. W. J.; van Delden, R. A.; Harada, N.; Feringa, B. L. Light-driven monodirectional molecular rotor. *Nature* **1999**, *401*, 152−155.
(11) Balzani, V.; Clemente-León, M.; Credi, A.; Ferrer, B.; Venturi, M.; Flood, A. H.; Stoddart, J. F. Autonomous artificial nanomotor powered by sunlight. *Proc. Natl. Acad. Sci. U. S. A.* **2006**, *103*, 1178−1183.
(12) Kelly, T. R.; Silva, R. A.; De Silva, H.; Jasmin, S.; Zhao, Y. Rationally designed prototype of a molecular motor. *J. Am. Chem. Soc.* **2000**, *122*, 6935−6949.
(13) Hernández, J. V.; Kay, E. R.; Leigh, D. A. A reversible synthetic rotary molecular motor. *Science* **2004**, *306*, 1532−1537.
(14) Fletcher, S. P.; Dumur, F.; Pollard, M. M.; Feringa, B. L. A reversible, unidirectional molecular rotary motor driven by chemical energy. *Science* **2005**, *310*, 80−82.
(15) Seldenthuis, J. S.; Prins, F.; Thijssen, J. M.; van der Zant, H. S. J. An all-electric single-molecule motor. *ACS Nano* **2010**, *4*, 6681−6686.
(16) Horinek, D.; Michl, J. Molecular dynamics simulation of an electric field driven dipolar molecular rotor attached to a quartz glass surface. *J. Am. Chem. Soc.* **2003**, *125*, 11900−11910.
(17) Kay, E. R.; Leigh, D. A.; Zerbetto, F. Synthetic molecular motors and mechanical machines. *Angew. Chem., Int. Ed.* **2007**, *46*, 72−191.
(18) *Macrocyclic and Supramolecular Chemistry*; Izatt, R. M., Ed.; John Wiley & Sons, Ltd.: New York, New York, 2016.
(19) Balzani, V.; Credi, A.; Venturi, M. *Molecular Devices and Machines: Concepts and Perspectives for the Nanoworld*; John Wiley & Sons, Ltd.: New York, New York, 2008.
(20) Kratky, C.; Waditschatka, R.; Angst, C.; Johansen, J. E.; Plaquevent, J. C.; Schreiber, J.; Eschenmoser, A. The saddle conformation of hydroporphinoid nickel(II) complexes: structure, origin, and stereochemical consequence. *Helv. Chim. Acta* **1985**, *68*, 1312−1337.
(21) Waditschatka, R.; Kratky, C.; Jaun, B.; Heinzer, J.; Eschenmoser, A. Chemistry of pyrrocorphins: structure of nickel(II)-ccccc-octaethyl-pyrrocorphinate in the solid state and in solution. observation of the inversion barrier between enantiomorphically ruffled conformers. *J. Chem. Soc., Chem. Commun.* **1985**, *304*, 1604−1607.
(22) Geno, M. K.; Halpern, J. Why does nature not use the porphyrin ligand in vitamin B12? *J. Am. Chem. Soc.* **1987**, *109*, 1238−1240.
(23) Furenlid, L. R.; Renner, M. W.; Smith, K. M.; Fajer, J. Structural consequences of nickel versus macrocycle reductions in F430 models: EXAFS studies of a Ni(I) anion and Ni(II) .pi. anion radicals. *J. Am. Chem. Soc.* **1990**, *112*, 1634−1635.
(24) Vrtis, R. N.; Rao, C. P.; Bott, S. G.; Lippard, S. J. Synthesis and stabilization of tantalum-coordinated dihydroxyacetylene from two reductively coupled carbon monoxide ligands. *J. Am. Chem. Soc.* **1988**, *110*, 7564−7566.
(25) Anderson, K. K.; Hobbs, J. D.; Luo, L.; Stanley, K. D.; Quirke, J. M. E.; Shelnutt, J. A. Planar-nonplanar conformational equilibrium in metal derivatives of octaethyl porphyrin and meso-nitrooctaethylporphyrin. *J. Am. Chem. Soc.* **1993**, *115*, 12346−12352.
(26) Shelnutt, J. A.; Medforth, C. J.; Berber, M. D.; Barkigia, K. M.; Smith, K. M. Relationships between structural parameters and raman frequencies for some planar and nonplanar nickel(II) porphyrins. *J. Am. Chem. Soc.* **1991**, *113*, 4077−4087.
(27) Medforth, C. J.; Dolores Berber, M.; Smith, K. M.; Shelnutt, J. A. Tetracycloalkenyl-meso-tetraphenylporphyrins as models for the effect of non-planarity on the light absorption properties of photosynthetic chromophores. *Tetrahedron Lett.* **1990**, *31*, 3719−3722.
(28) Zhang, Q.; Zheng, X.; Kuang, G.; Wang, W.; Zhu, L.; Pang, R.; Shi, X.; Shang, X.; Huang, X.; Liu, P.; Lin, N. Single-molecule investigations of conformation adaptation of porphyrins on surfaces. *J. Phys. Chem. Lett.* **2017**, *8*, 1241−1247.
(29) Costa, S. M. B.; Velázquez, M. M.; Tamai, N.; Yamazaki, I. Luminescence of porphyrins: relevance to electron transfer processes. *J. Lumin.* **1991**, *48*−*49*, 341−351.
(30) Harriman, A. Luminescence of porphyrins and metalloporphyrins. part 1.-zinc(II), nickel(II) and manganese(II) porphyrins. *J. Chem. Soc., Faraday Trans. 1* **1980**, *76*, 1978−1985.
(31) Harriman, A. Luminescence of porphyrins and metalloporphyrins. part 2.-copper(II), chromium(III), manganese(III), iron(II) and iron(III) porphyrins. *J. Chem. Soc., Faraday Trans. 1* **1981**, *77*, 369−377.
(32) Kuang, G.; Zhang, Q.; Lin, T.; Pang, R.; Shi, X.; Xu, H.; Lin, N. Mechanically-controlled reversible spin crossover of single Fe-porphyrin molecules. *ACS Nano* **2017**, *11*, 6295−6300.
(33) Ali, Md. E.; Sanyal, B.; Oppeneer, P. M. Electronic structure, spin-states, and spin-crossover reaction of heme-related Fe-porphyrins: a theoretical perspective. *J. Phys. Chem. B* **2012**, *116*, 5849−5859.
(34) Iancu, V.; Deshpande, A.; Hla, S.-W. Manipulating Kondo temperature via single molecule switching. *Nano Lett.* **2006**, *6*, 820−823.
(35) Kim, H.; Chang, Y. H.; Lee, S.-H.; Kim, Y.-H.; Kahng, S.-J. Switching and sensing spin states of Co-porphyrin in bimolecular reactions on Au(111) using scanning tunneling microscopy. *ACS Nano* **2013**, *7*, 9312−9317.
(36) Kuang, G.; Zhang, Q.; Li, D.; Shang, X.; Lin, T.; Liu, P.; Lin, N. Cross-coupling of aryl-bromide and porphyrin-bromide on an Au (111) surface. *Chem. - Eur. J.* **2015**, *21*, 8028−8032.
(37) Kottas, G. S.; Clarke, L. I.; Horinek, D.; Michl, J. Artificial molecular rotors. *Chem. Rev.* **2005**, *105*, 1281−1376.
(38) Tashiro, K.; Konishi, K.; Aida, T. Enantiomeric resolution of chiral metallobis(porphyrin)s: studies on rotatability of electronically coupled porphyrin ligands. *Angew. Chem., Int. Ed. Engl.* **1997**, *36*, 856−858.
(39) Vacek, J.; Michl, J. Artificial surface-mounted molecular rotors: molecular dynamics simulations. *Adv. Funct. Mater.* **2007**, *17*, 730−739.
(40) Vaughan, O. P. H.; Williams, F. J.; Bampos, N.; Lambert, R. M. A chemically switchable molecular pinwheel. *Angew. Chem., Int. Ed.* **2006**, *45*, 3779−3781.
(41) Tanaka, H.; Ikeda, T.; Takeuchi, M.; Sada, K.; Shinkai, S.; Kawai, T. Molecular Rotation in Self-Assembled Multidecker Porphyrin Complexes. *ACS Nano* **2011**, *5*, 9575−9582.
(42) Zhang, Y.; Kersell, H.; Stefak, R.; Echeverria, J.; Iancu, V.; Perera, U. G. E.; Li, Y.; Deshpande, A.; Braun, K.-F.; Joachim, C.; Rapenne, G.; Hla, S.-W. Simultaneous and coordinated rotational switching of all molecular rotors in a network. *Nat. Nanotechnol.* **2016**, *11*, 706−712.
(43) Senge, M. O.; MacGowan, S. A.; O'Brien, J. M. Conformational control of cofactors in nature − the influence of protein-induced macrocycle distortion on the biological function of tetrapyrroles. *Chem. Commun.* **2015**, *51*, 17031−17063.
(44) Dong, L.; Gao, Z.; Lin, N. Self-assembly of metal-organic coordination structures on surfaces. *Prog. Surf. Sci.* **2016**, *91*, 101−135.

https://dx.doi.org/10.1021/acs.jpcb.9b09986
J. Phys. Chem. B 2020, 124, 953−960

(45) Zhang, Q.; Kuang, G.; Pang, R.; Shi, X.; Lin, N. Switching molecular Kondo effect via supramolecular interaction. *ACS Nano* **2015**, *9*, 12521−12528.
(46) Zhao, R.; Qi, F.; Zhao, Y.; Hermann, K.; Zhang, R.; Van Hove, M. A. Interlocking molecular gear chains built on surfaces. *J. Phys. Chem. Lett.* **2018**, *9*, 2611−2619.
(47) Zhao, R.; Zhao, Y.; Qi, F.; Hermann, K.; Zhang, R.; Van Hove, M. A. Interlocking mechanism between molecular gears attached to surfaces. *ACS Nano* **2018**, *12*, 3020−3029.
(48) Yan, L.; Hua, M.; Zhang, Q.; Ngai, T. U.; Guo, Z.; Wu, T. C.; Wang, T.; Lin, N. Symmetry breaking in molecular artificial graphene. *New J. Phys.* **2019**, *21*, 083005.
(49) Jarvis, S. P.; Taylor, S.; Baran, J. D.; Thompson, D.; Saywell, A.; Mangham, B.; Champness, N. R.; Larsson, J. A.; Moriarty, P. Physisorption controls the conformation and density of states of an adsorbed porphyrin. *J. Phys. Chem. C* **2015**, *119*, 27982−27994.
(50) Müllegger, S.; Rashidi, M.; Lengauer, T.; Rauls, E.; Schmidt, W. G.; Knör, G.; Schöfberger, W.; Koch, R. Asymmetric saddling of single porphyrin molecules on Au(111). *Phys. Rev. B: Condens. Matter Mater. Phys.* **2011**, *83*, 165416.
(51) Albrecht, F.; Bischoff, F.; Auwärter, W.; Barth, J. V.; Repp, J. Direct identification and determination of conformational response in adsorbed individual nonplanar molecular species using noncontact atomic force microscopy. *Nano Lett.* **2016**, *16*, 7703−7709.
(52) Kresse, G.; Furthmüller, J. Efficient iterative schemes for ab initio total-energy calculations using a plane-wave basis set. *Phys. Rev. B: Condens. Matter Mater. Phys.* **1996**, *54*, 11169−11186.
(53) Kresse, G.; Joubert, D. From ultrasoft pseudopotentials to the projector augmented-wave method. *Phys. Rev. B: Condens. Matter Mater. Phys.* **1999**, *59*, 1758−1775.
(54) Klimeš, J.; Bowler, D. R.; Michaelides, A. Van der waals density functionals applied to solids. *Phys. Rev. B: Condens. Matter Mater. Phys.* **2011**, *83*, 195131.
(55) Wang, W.; Pang, R.; Kuang, G.; Shi, X.; Shang, X.; Liu, P.; Lin, N. Intramolecularly resolved Kondo resonance of high-spin Fe(II)-porphyrin adsorbed on Au(111). *Phys. Rev. B: Condens. Matter Mater. Phys.* **2015**, *91*, 045440.
(56) Klappenberger, F.; Weber-Bargioni, A.; Auwärter, W.; Marschall, M.; Schiffrin, A.; Barth, J. V. Temperature dependence of conformation, chemical state, and metal-directed assembly of tetrapyridyl-porphyrin on Cu(111). *J. Chem. Phys.* **2008**, *129*, 214702.
(57) Buchner, F.; Zillner, E.; Röckert, M.; Gläßel, S.; Steinrück, H.-P.; Marbach, H. Substrate-mediated phase separation of two porphyrin derivatives on Cu (111). *Chem. - Eur. J.* **2011**, *17*, 10226−10229.
(58) Furukawa, M.; Tanaka, H.; Sugiura, K.; Sakata, Y.; Kawai, T. Fabrication of molecular alignment at the specific sites on Cu(111) surfaces using self-assembly phenomena. *Surf. Sci.* **2000**, *445*, 58−63.
(59) Becke, A. D.; Edgecombe, K. E. A simple measure of electron localization in atomic and molecular systems. *J. Chem. Phys.* **1990**, *92*, 5397−5403.
(60) Fleischer, E. B.; Wang, J. H. The detection of a type of reaction intermediate in the combination of metal ions with porphyrins. *J. Am. Chem. Soc.* **1960**, *82*, 3498−3502.
(61) Brand, H.; Arnold, J. Recent developments in the chemistry of early transition metal porphyrin compounds. *Coord. Chem. Rev.* **1995**, *140*, 137−168.
(62) Adler, A.; Longo, F.; Shergalis, W. Mechanistic investigations of porphyrin syntheses. I. preliminary studies on ms-tetraphenylporphin. *J. Am. Chem. Soc.* **1964**, *86*, 3145−3149.
(63) Diller, K.; Papageorgiou, A. C.; Klappenberger, F.; Allegretti, F.; Barth, J. V.; Auwärter, W. In vacuo interfacial tetrapyrrole metalation. *Chem. Soc. Rev.* **2016**, *45*, 1629−1656.
(64) Cotton, T. M.; Schultz, S. G.; Van Duyne, R. P. Surface-enhanced resonance raman scattering from water-soluble porphyrins adsorbed on a silver electrode. *J. Am. Chem. Soc.* **1982**, *104*, 6528−6532.
(65) Auwärter, W.; Weber-Bargioni, A.; Brink, S.; Riemann, A.; Schiffrin, A.; Ruben, M.; Barth, J. V. Controlled metalation of self-assembled porphyrin nanoarrays in two dimensions. *ChemPhysChem* **2007**, *8*, 250−254.
(66) Le Gac, S.; Furet, E.; Roisnel, T.; Hijazi, I.; Halet, J.-F.; Boitrel, B. A pentanuclear lead(II) complex based on a strapped porphyrin with three different coordination modes. *Inorg. Chem.* **2014**, *53*, 10660−10666.
(67) John Plater, M; Aiken, S.; Bourhill, G. Metallated porphyrins containing lead(II), copper(II) or zinc(II). *Tetrahedron* **2002**, *58*, 2415−2422.
(68) Plater, M. J.; Aiken, S.; Gelbrich, T.; Hursthouse, M. B.; Bourhill, G. Structures of Pb(II) porphyrins: [5,10,15,20-tetrakis-triisopropylsilylethynylporphinato]lead(II) and [5,15-bis-(3,5-bis-tert-butylphenyl)-10,20-bis-triisopropylsilylethynylporphinato]lead(II). *Polyhedron* **2001**, *20*, 3219−3224.
(69) Sperl, A.; Kröger, J.; Berndt, R. Electronic superstructure of lead phthalocyanine on lead islands. *J. Phys. Chem. A* **2011**, *115*, 6973−6978.
(70) Castellanos-Gomez, A.; van Wees, B. J. Band gap opening of graphene by noncovalent π-π interaction with porphyrins. *Graphene* **2013**, *2*, 102−108.
(71) Aly, S. M.; Parida, M. R.; Alarousu, E.; Mohammed, O. F. Ultrafast electron injection at the cationic porphyrin−graphene interface assisted by molecular flattening. *Chem. Commun.* **2014**, *50*, 10452−10455.
(72) Geng, J.; Kong, B.; Yang, S. B.; Jung, H. Preparation of graphene relying on porphyrin exfoliation of graphite. *Chem. Commun.* **2010**, *46*, 5091−5093.
(73) Pham, V. D.; Joucken, F.; Repain, V.; Chacon, C.; Bellec, A.; Girard, Y.; Rousset, S.; Sporken, R.; Santos, M. C. d.; Lagoute, J. Molecular adsorbates as probes of the local properties of doped graphene. *Sci. Rep.* **2016**, *6*, 24796.
(74) Gadipelli, S.; Guo, Z. X. Graphene-based materials: synthesis and gas sorption, storage and separation. *Prog. Mater. Sci.* **2015**, *69*, 1−60.
(75) Bakar, M. B.; Oelgemöller, M.; Senge, M. O. Lead structures for applications in photodynamic therapy. part 2: synthetic studies for photo-triggered release systems of bioconjugate porphyrin photo-sensitizers. *Tetrahedron* **2009**, *65*, 7064−7078.
(76) Morales Vasquez, M. A.; Suarez, S. A.; Doctorovich, F. Gold and silver anchored cobalt porphyrins used for catalytic water splitting. *Mater. Chem. Phys.* **2015**, *159*, 159−166.

https://dx.doi.org/10.1021/acs.jpcb.9b09986
J. Phys. Chem. B 2020, 124, 953−960